Creep Resistance and High-Temperature Metallurgical Stability of Titanium Alloys Containing Gallium

C. E. SHAMBLEN AND T. K. REDDEN

Tensile properties up to 1100°F and the creep resistance at 1000°F were correlated with composition for twelve complex developmental titanium alloys with additions of Al, Ga, Sn, Mo, Zr, and Si. Creep resistance for these alloys in the β heat-treated condition was found to be strongly dependent on the total α stabilizer content and the silicon concentration. The creep activation energy for a Ti-4.5 Al-2 Sn-3 Zr-3 Ga-1 Mo-0.5 Si alloy, established over the 900° to 1100°F temperature range, was about 100 kcal per g-mole. This high creep activation energy is hypothesized to result from dispersion strengthening within the α matrix by the Ti_3X (X = Al, Ga, Sn) phase and pinning of the interplatelet and prior β grain boundaries by the Zr_5Si_3 phase. Both phases were identified by transmission electron microscopy in these respective locations. Metallurgical instability, as evidenced by decreased fracture toughness, is also shown to be relatable to the total α stabilizer content. The activation energy for the embrittlement process is about 45 kcal per g-mole. which approximates that for interdiffusion of gallium in α titanium.

THE mechanical properties of commercial and recent development alloys indicate that the next generation of high-temperature (800° to 1200°F) titanium alloys will be based on the silicon bearing, near-α system. The major technical problem for this system is achieving high-temperature strength without significantly compromising metallurgical stability. Metallurgical stability is defined as the ability to retain adequate low temperature toughness after long-time thermal exposure at 800° to 1200°F. The embrittlement of these alloys is believed to be associated with the Ti_3X phase, where X designates the α stabilizing elements Al, Ga, and Sn. Crossley and Carew[1] initially reported this type of embrittlement for a Ti-8 wt pct Al alloy in 1957. This behavior was confirmed by Soltis[2] and attributed to the ordered Ti_3Al phase in the commercial Ti-8 Al-1 Mo-1 V alloy. More recently, Shamblen[3] conducted a kinetic analysis of the embrittlement for the Ti-6 Al-2 Sn-4 Zr-2 Mo and Ti-5 Al-6 Sn-2 Zr-1 Mo-0.25 Si alloys to link the toughness degradation activation energy with that for interdiffusion of aluminum and tin in titanium. Although there is a lack of agreement on the Ti-Al phase diagram,[4-7] the existence of an ordered Ti_3Al phase with the DO_{19} structure is generally acknowledged. The Ti-Sn and Ti-Ga systems[8] are similarly recognized to exhibit Ti_3X phases with the DO_{19} structure which are assumed isomorphous with the Ti_3Al phase. Ti_3X is the initial intermediate phase for these three systems which results in limitation of the α solubility of these elements.

Alpha stabilizing elements, such as Al, Ga, or Sn, do promote high-temperature strength in titanium alloys by solid solution strengthening. However, Rosenberg[9] has shown that aluminum additions in binary Ti-Al alloys must be limited to less than 9 wt pct to avoid the embrittlement associated with the Ti_3Al phase. Jepson[10] recently presented evidence showing a significant strength improvement for binary titanium alloys due to additions of gallium. Gallium was found to be about 80 pct as effective as aluminum on a wt pct basis for increasing the creep and rupture strength of titanium alloys, whereas the more commercially applied tin addition is only about 30 pct as effective as aluminum. Gallium was believed to exhibit the further advantage of allowing significant solid solution strengthening prior to metallurgical stability problems with the Ti_3Ga phase based on the earlier phase diagram showing 14 to 15 wt pct solubility for the α phase at 1200°F. However, Shamblen and Rosa[11] in a study concurrent with the present investigation found the α titanium solubility of gallium was actually only about 7 wt pct at 1200°F.

Twelve titanium-base alloys, most of which contain gallium with other additions of Al, Sn, Mo, Zr, and Si based on the current alloy design practice, were evaluated in this study. The advantages of the α stabilizing elements were described, whereas small additions of the β stabilizer, molybdenum, were used to impart superior elevated temperature tensile strength. The zirconium and silicon additions in titanium alloys have been shown[12] to interact to form a silicide phase which significantly increases elevated temperature creep resistance. Silicon solubility is greater in β titanium than α titanium such that β heat treatments were used to solution the silicon with a subsequent stabilization age at 1100°F for 2 hr to acquire a silicide dispersion. The microconstituents after β heat treatment of these α stabilized alloys consist of a basket-weave α microstructure with orientation relationship to the prior β grains, the Ti_3X phase within the basket-weave α plates and the silicide phase. The alloys containing molybdenum may also exhibit a minor retained β phase content. Preliminary evaluations of the tensile properties, creep resistance, and metallurgical stability were conducted to select a superior alloy which was then evaluated in further detail.

C. E. SHAMBLEN and T. K. REDDEN are Metallurgist and Manager–Titanium Alloys, respectively, Material and Process Technology Laboratories, Aircraft Engine Group, General Electric Co., Cincinnati, Ohio.

Manuscript submitted August 12, 1971.

EXPERIMENTAL

Alloy Design

Twelve developmental alloys were consumable-electrode, double-arc melted under vacuum as 25 lb. ingots with the chemical compositions shown in Table I. The alloys are separated into five series in Table I to identify variations in the Ga, Al, Si, and Mo levels. The fifth series consists of two alloys with variations in both the gallium and aluminum levels. The tin and zirconium levels were maintained constant in all twelve alloys. The A1 and A2 alloys are repeated as necessary in Table I to complete the various series. The alloy composition levels were designed on an empirical aluminum equivalent basis[9] which has been used to predict the "safe" composition envelope precluding severe embrittlement as a result of metallurgical instability. The aluminum equivalent formula in terms of wt pct additions as originally proposed is:

$$(Al) + \tfrac{1}{3}(Sn) + \tfrac{1}{6}(Zr) + 10(O_2) \leq 9 \qquad [1]$$

However, recent unpublished studies at the authors' laboratory have indicated that the "safe" aluminum equivalent is likely ≤ 8 for this formula. The above concept was used to develop the compositions shown in Table I, with a value of $\frac{1}{2}$ estimated as the factor for gallium. The $\frac{1}{2}$ factor is an empirical estimate based on the earlier reported solubility of gallium, in wt pct, being approximately twice that for aluminum. The average oxygen level for each of the twelve heats was 0.07 wt pct. The aluminum equivalents, with the addition of the gallium term to Eq. [1], are shown in Table I. All of the alloys, except D1 and D2, remain within the "safe" composition envelope based on these calculations. Recognizing the $\frac{1}{2}$ factor for gallium is only an assumption, the D1 alloy was designed to exceed the aluminum equivalent value of 8. The D2 alloy was designed to verify the instability results at the aluminum equivalent level of about 9 without a gallium addition.

Table I. Development Alloy Compositions

Alloy No.	Ga	Al	Sn	Zr	Si	Mo	Aluminum Equivalent	β Transus, °F ± 10°F
				Gallium Series				
A1	–	4,5	2	3	0.5	–	6.4	1815
A2	3	4.5	2	3	0.5	–	7.9	1815
D1	7	4.5	2	3	0.5	–	9.9	1840
				Aluminum Series				
(A1)	–	4.5	2	3	0.5	–	6.4	1815
D3	–	6	2	3	0.5	–	7.9	1865
D2	–	7	2	3	0.5	–	8.9	1890
				Silicon Series				
B1	3	4.5	2	3	–	–	7.9	1815
B2	3	4.5	2	3	0.3	–	7.9	1815
(A2)	3	4.5	2	3	0.5	–	7.9	1815
B3	3	4.5	2	3	0.7	–	7.9	1815
				Molybdenum Series				
(A2)	3	4.5	2	3	0.5	–	7.9	1815
C1	3	4.5	2	3	0.5	1	7.9	1815
C2	3	4.5	2	3	0.5	2	7.9	1790
				Gallium/Aluminum Variation Series				
A3	5	3.5	2	3	0.5	–	7.9	1790
A4	7	2.5	2	3	0.5	–	7.9	1765

Alloy Processing and Testing

The development alloys were initially β processed by extrusion to 1.5 in. diam bar. The β transus temperatures were determined, as shown in Table I, and the materials were swaged to 0.5 in. diam at approximately 40°F below the β transus. The alloys were subsequently heat treated at ~100°F above the transus for 1 hr, air cooled and then stabilized at 1100°F for 2 hr.

Standard tensile, creep, and post-creep-exposure tensile tests with the oxide layer intact were conducted on the twelve alloys. In addition, thermally exposed fatigue precracked Charpy bar specimens were slow bend tested to evaluate metallurgical stability. The quantitative measurement obtained from testing the fatigue precracked Charpy specimen was a K_c value calculated by the standard ASTM procedure used for K_{Ic} bend specimens. The K_c value is simply considered a mixed mode stress intensity factor (ksi $\sqrt{\text{in.}}$).

RESULTS AND ANALYSIS

β Transus Determination

The metallographically determined β transus values, shown in Table I, are empirically correlatable as a function of wt pct composition to give the following equation:

$$\beta_t(°F) = 1640 + 37(Al) + 2.5(Ga) - 8(Mo) \qquad [2]$$

The antimony, zirconium, and interstitial contents of the base composition are assumed to account for the increase in the β transus from the 1620°F value for unalloyed titanium to 1640°F since the multipliers for tin and zirconium are negative while those for C, O, and N are positive. Silicon in the range of 0 to 0.7 wt pct had no observable effect on the β transus temperature.

Tensile Properties

Standard tensile tests were conducted at room temperature, 700°, 900°, and 1100°F. The tensile data for room temperature and 900°F are shown in Table II and all the 0.2 pct yield strength data for the Ga, Al, Mo, and Si series are summarized on Fig. 1. The wt pct strengthening coefficients were calculated for each of these elements to develop the following formulae for the Ti-2 Sn-3 Zr-0.07 O_2 base. The open data points in Fig. 1 contain a correction factor for a second element besides the major element being considered. For example, the 5 wt pct Ga alloy (A3) actually contains only 3.5 wt pct Al, and 6 ksi is added to the room temperature strength value to consider this gallium level with the 4.5 Al-2 Sn-3 Zr-0.5 Si base. The strength values for the base alloy, Ti-2 Sn-3 Zr-0.07 O_2, are the result of calculations considering all twelve alloys.

Room Temperature

$$0.2 \text{ pct YS (ksi)} = (75.0 \pm 3.0) + 4.3(Ga) + 6.0(Al) + 14(Mo) + 30(Si) \qquad [3]$$

700°F

$$0.2 \text{ pct YS (ksi)} = (37.7 \pm 2.8) + 3.4(Ga) + 3.7(Al) + 14(Mo) + 24(Si) \qquad [4]$$

900°F

$$0.2 \text{ pct YS (ksi)} = (32.6 \pm 1.3) + 3.2(\text{Ga}) + 3.4(\text{Al}) + 14(\text{Mo}) + 24(\text{Si}) \quad [5]$$

1100°F

$$0.2 \text{ pct YS (ksi)} = (31.6 \pm 1.7) + 2.8(\text{Ga}) + 3.2(\text{Al}) + 14(\text{Mo}) + 24(\text{Si}) \quad [6]$$

Ductility trends were generally inversely proportional to the strength level, although the D1 alloy, with the aluminum equivalent of 9.9, demonstrated extremely brittle behavior at room temperature.

Creep Resistance

Constant load creep tests were conducted on the developmental alloys at 900°, 950°, and 1000°F. The data for these alloys approximated the classical three stage creep process. However, an extended duration was noted for the primary creep stage, *i.e.*, that of a decreasing rate of plastic deformation, which is assumed to be related to the continued formation or growth of the Ti_3X or silicide phases during the creep test. The tests were generally in the constant rate second stage creep when terminated for tensile test. The alloy comparison can be conveniently summarized with just the results for the time to 0.2 pct plastic creep at 1000°F and 55 ksi. Superior creep resistance with increased alloy content was observed for the Ga, Al, and Si additions. A 1 wt pct Mo addition improved creep resistance, but the 2 wt pct Mo alloy exhibited creep properties inferior to that for the 1 wt pct Mo alloy.

The major factors influencing creep resistance in these titanium alloys were found to be the summation of the α stabilizer content, the silicon level and to some extent the elevated temperature yield strength. The effect of the first two factors on the creep resistance is

Table II. Tensile Properties at Room Temperature and 900°F

		Room Temperature			900°F		
Gallium Series	Ga	0.2 pct YS, ksi	UTS ksi	RA pct	0.2 pct YS, ksi	UTS ksi	RA pct
A1	–	119	129	24	62	75	33
A2	3	132	144	25	70	84	32
D1	7	–	128	0	83	100	29
Aluminum Series	Al						
(A1)	4.5	119	129	24	62	75	33
D3	6	125	135	23	67	84	29
D2	7	129	142	24	69	86	28
Silicon Series	Si						
B1	–	116	126	28	59	74	39
B2	0.3	122	134	30	66	82	35
(A2)	0.5	132	144	25	70	84	32
B3	0.7	137	148	21	76	90	28
Molybdenum Series	Mo						
(A2)	–	132	144	25	70	84	32
C1	1	146	160	15	92	111	25
C2	2	148	173	12	98	131	17
Gallium/Aluminum Variation Series							
A3		132	142	14	71	87	33
A4		139	150	22	73	90	31

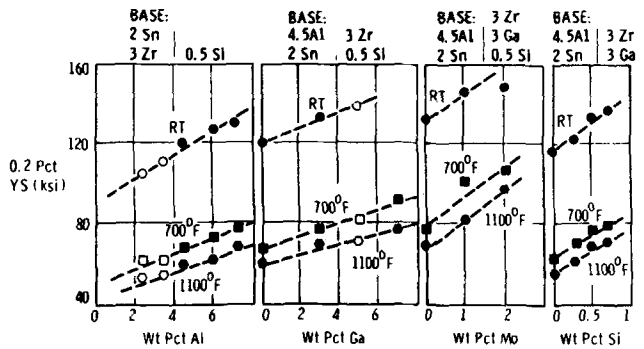

Fig. 1—Effect of Al, Ga, Mo, and Si on the 0.2 pct yield strength of titanium alloys.

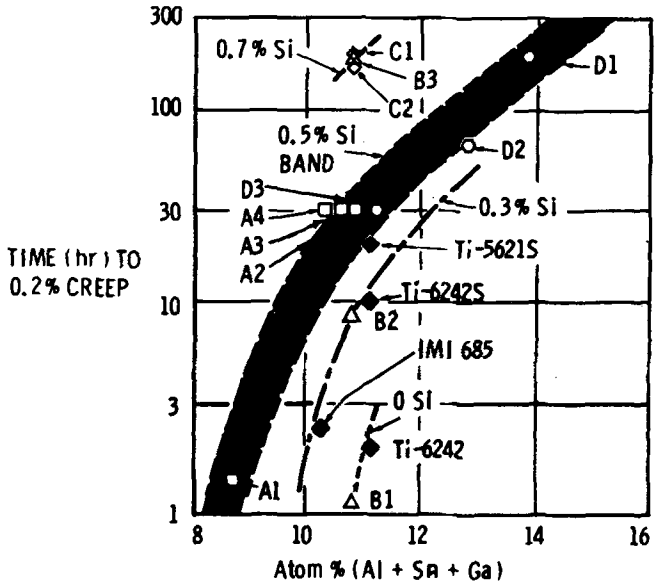

Fig. 2—Effect of the α stabilizing elements on the creep resistance of titanium alloys at constant silicon levels (creep conditions: 1000°F/55 ksi).

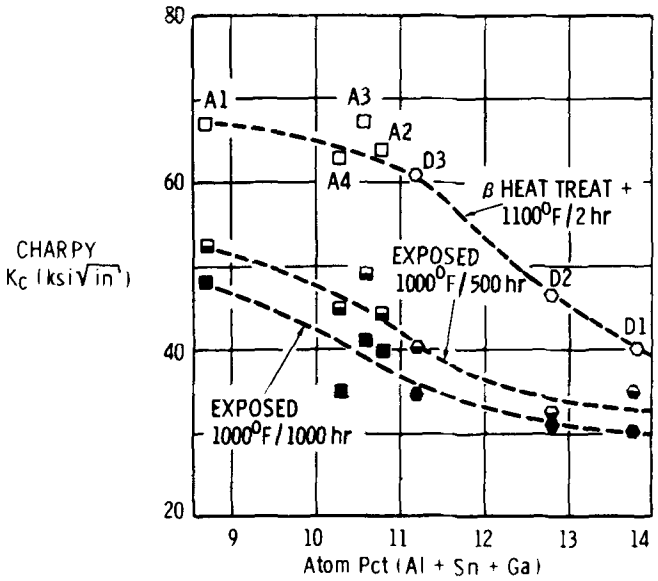

Fig. 3—Effect of the α stabilizing elements on the stability of titanium alloys.

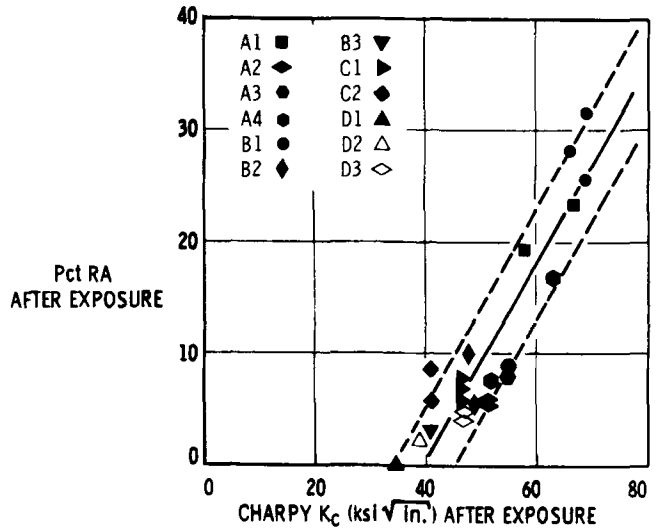

Fig. 4—β heat treatment post-creep ductility correlation to Charpy K_C toughness data.

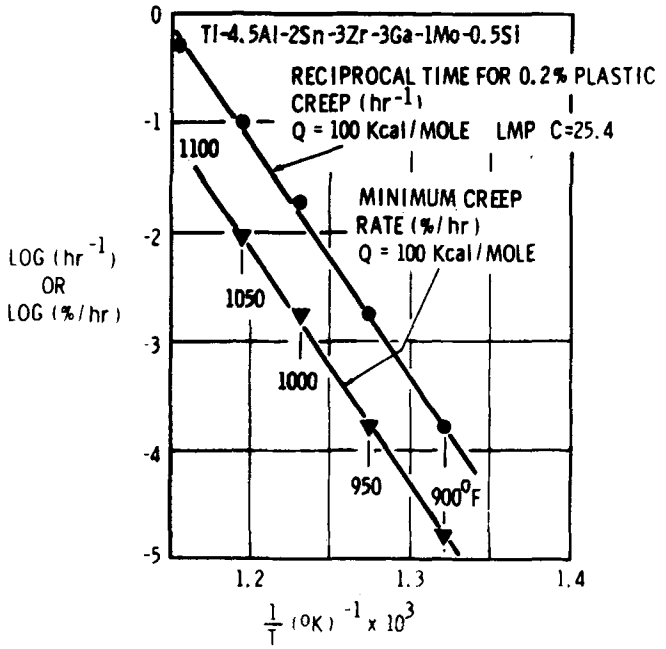

Fig. 5—Creep activation energy for the C1 alloy at 60 ksi.

established in Fig. 2 where the time to 0.2 pct plastic creep is plotted vs the summation of the at. pct of the α stabilizers. The results separate in distinct bands for the various silicon levels of 0, 0.3, 0.5, and 0.7 wt pct. Supplementary data on the commercial alloys Ti-6 Al-2 Sn-4 Zr-2 Mo (Ti-6242), Ti-6 Al-2 Sn-4 Zr-2 Mo-0.25 Si (Ti-6242S), Ti-6 Al-5 Zr-0.5 Mo-0.25 Si (IMI 685), and Ti-5 Al-6 Sn-2 Zr-1 Mo-0.25 Si (Ti-5621S) have been used to further describe these compositional effects. The creep results for the developmental C1 and C2 alloys, which both contain molybdenum additions and have a value of 10.8 at. pct (Al + Ga + Sn), are considerably displaced to longer times to 0.2 pct plastic creep in Fig. 2. The results for C1 and C2 fall on the 0.7 wt pct Si curve even though they contain only 0.5 wt pct Si. This effect is believed to be related to the higher elevated temperature yield strength resulting from the molybdenum addition.

Stability

The metallurgical stability of the alloys was evaluated by two test methods: the subsize fracture mechanics evaluation consisting of a slow bend test of a thermally exposed fatigue precracked Charpy bar and the earlier method of the post-creep tensile ductility test.

The K_C fracture toughness values are summarized in Fig. 3 for the as-heat-treated condition and after exposure at 1000°F. A comparison is made of the fatigue precracked Charpy K_C (ksi $\sqrt{in.}$) value vs the atomic percent summation of Al + Ga + Sn. The molybdenum and silicon variation alloys were not considered for this correlation. A definite trend of decreased toughness with increasing α stabilizer content exists. The effect of silicon and molybdenum on metallurgical stability is proposed to be related to reduced toughness resulting from the higher strength of these alloys. Since fracture toughness is generally inversely related to strength, molybdenum and silicon additions, which are potent strengtheners, reduce the initial toughness prior to exposure and give an apparent decrease in stability without actually effecting a change in the causative metallurgical reaction. Metallurgical instability is considered attributable to the formation and growth of the Ti_3X (X = Al, Ga, Sn) phase.

The correlation of the post creep exposure ductility results for the twelve developmental alloys with the K_C values for equivalent thermal exposure times at 1000°F is shown in Fig. 4. The plot of the percent RA vs the Charpy K_C shows that when K_C is degraded to the range of 40 ksi $\sqrt{in.}$, the tensile ductility will be between 0 and 6 pct RA. Therefore, the post creep tensile test limit for a detectable difference in stability with a 0.250 in. diam titanium alloy tensile bar in the β heat-treatment condition is the K_C value of 40 ksi $\sqrt{in.}$, whereas differences below this value can adequately be defined using the Charpy bar test.

Extended Study of the C1 Alloy

A review of the results for the twelve alloys shows that the C1 composition, Ti-4.5 Al-2 Sn-3 Zr-3 Ga-1 Mo-0.5 Si, exhibits superior tensile and creep resistance properties. Although this alloy exhibits some degree of metallurgical instability, it merited further study. Constant load creep tests were conducted at 60 ksi over the temperature range of 900° to 1100°F to establish the creep activation energy and the associated Larson-Miller[13] parameter constant. Creep in metals has been shown to be a thermally activated process which can be described at a constant stress level by an Arrhenius equation of the form:

$$\text{Rate} = \frac{1}{t} = A \exp\left[-Q/RT\right] \qquad [7]$$

The Larson-Miller concept of analyzing creep data is an extension of the Arrhenius rate equation for expressing the stress dependence of the activation energy, Q, and may be stated in the form:

$$P = T(C + \log t) \qquad [8]$$

where P is equal to $Q/2.3(0.556)(1.986)$ or $Q/2.54$ for Q expressed in cal per g-mole. As P varies with stress, so therefore Q also varies with stress. The Arrhenius-type plots of log reciprocal time (hr^{-1}) to

0.2 pct plastic creep and the log minimum creep rate (pct per hr) vs the reciprocal absolute temperature (K^{-1}) are shown in Fig. 5. The creep activation energy was found to be about 100 kcal per g-mole at 60 ksi and extrapolation to $1/T = 0$, *i.e.*: an infinite temperature, indicated the applicable Larson-Miller constant was about 25. The creep data for the C1 alloy, at the 60 ksi and other stress levels, were then summarized by plotting the creep stress vs the Larson-Miller parameter as shown in Fig. 6. For stresses between 25 and 85 ksi, Q is seen to vary between 88 and 101 kcal per g-mole. The creep resistance of this alloy is shown in comparison to the current most creep resistant commercial alloy, Ti-5 Al-6 Sn-2 Zr-1 Mo-0.25 Si, in Fig. 6.

A detailed study of the time-temperature relationship of the toughness degradation using the fatigue precracked Charpy specimens was conducted for the C1 alloy. The results have been summarized in terms of the Wert-Zener[14] equation in Fig. 7 in the manner applied earlier[3] for the Ti-6 Al-2 Sn-4 Zr-2 Mo and Ti-5 Al-6 Sn-2 Zr-1 Mo-0.25 Si alloys. The Wert-Zener equation describes the kinetics for the diffusion controlled growth of a second phase of a different composition from that of the matrix. The equation and assumptions used for its application are as follows:

$$X_t = 1 - e^{-(t/\tau)^m} \qquad [9]$$

where:

X_t is generally considered as the volume fraction of a second phase, in this case Ti_3X

t = time

τ = time to 63 pct completion of the reaction

m = constant which was found to be approximately 0.41 for Ti-6 Al-2 Sn-4 Zr-2 Mo and Ti-5 Al-6 Sn-2 Zr-1 Mo-0.25 Si

The major assumption for this analysis is that the fractional toughness loss, X_t', is proportional to the volume fraction of the second phase (Ti_3X) and can be substituted directed for X_t.

The Wert-Zener equation was manipulated to the form:

$$\log [\ln 1/(1 - X_t')] = m \log t - m \log \tau \qquad [10]$$

for presentation in Fig. 7, where m is the slope of the $\ln 1°(1 - X_t')$ vs t plot with log-log coordinates, and τ is the intercept for $\ln 1/(1 - X_t')$ equal to unity. The statistical average m value for the least squares straight line slopes of these lines is 0.40, in close agreement with that for the two commercial titanium alloys studied earlier. The extrapolated τ values are shown in Fig. 7. The reciprocals to the τ values were then used to determine the activation energy for the embrittlement process in an Arrhenius plot as shown in Fig. 8. Again, a least-squares analysis was used to obtain the activation energy value of 45 kcal per g-mole, which is much higher than the 26 to 28 kcal per g-mole values found for the commercial alloys.

Light microscopy and electron transmission microscopy studies accompanied the evaluation of the C1

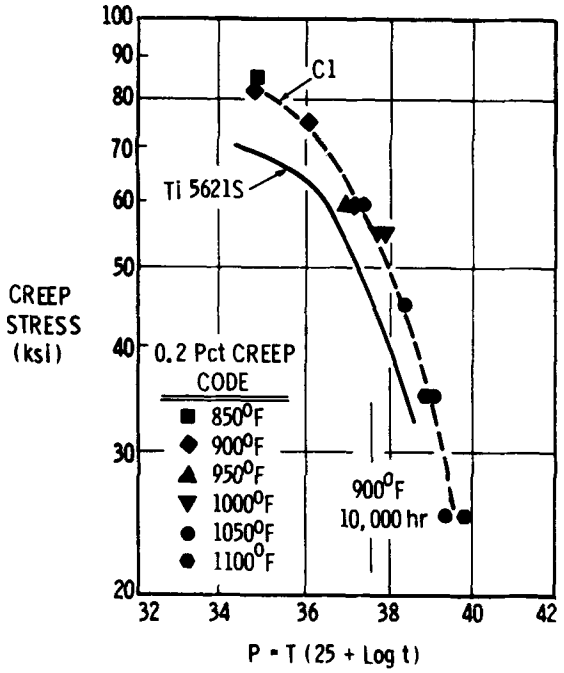

Fig. 6—Larson-Miller parameter 0.2 pct plastic creep curves for the C1 and Ti-5621S alloys.

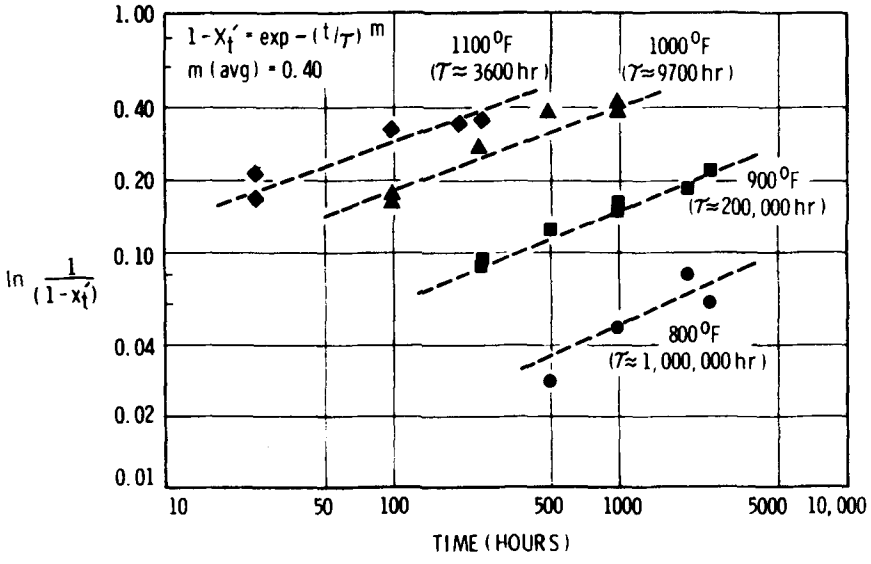

Fig. 7—Toughness loss for the C1 alloy as a function of time and temperature.

alloy. The Ti_3X (where X = Al, Ga, Sn) ordered phase is proposed to appear in spinoidal fashion in the alloy matrix, and the Zr_5Si_3 phase is found in the interplatelet and prior β grain boundaries as shown in Fig. 9.

DISCUSSION OF THE RESULTS

Since the summation of the atomic percent of the α stabilizing elements and the silicon content are dominant factors in achieving superior creep resistance, these factors can be used to propose a mechanism for the high creep activation energy observed for the C1 alloy. The creep activation energy for pure metals is generally accepted to be that for self diffusion. However, the alloys in this study cannot be considered pure metals or even single solid solutions. The alloys are in fact multiphase and we can hypothesize that the Ti_3X phase retards dislocation movement in the α matrix and that the Zr_5Si_3 phase in the interplatelet and prior β grain boundaries retards grain boundary sliding as a creep mechanism. These two factors, taken together, may explain the creep activation energy in the range of 88 to 101 kcal per g-mole, which is considerably higher than that estimated for self diffusion of titanium (60 kcal per g-mole). Both the Ti_3X and Zr_5Si_3 phases were identified in the C1 alloy in these respective locations.

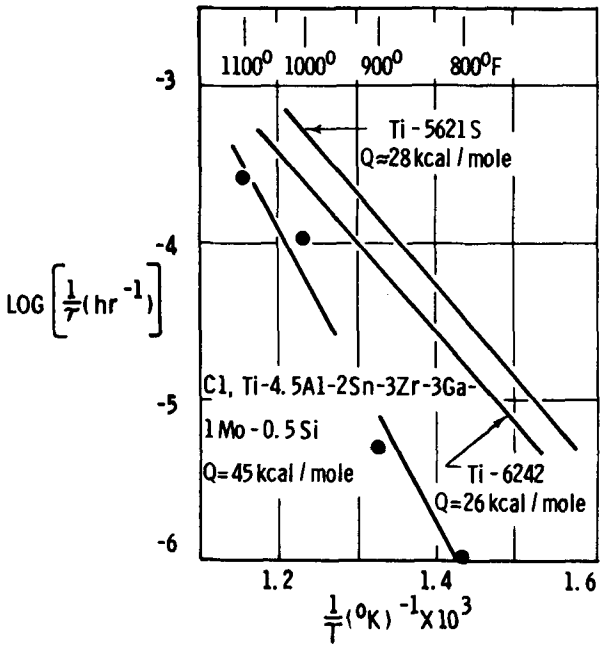

Fig. 8—Activation energy analysis for the C1 alloy metallurgical instability.

The stability of the gallium containing alloys was not as good as had been expected. However, the poorer results could have been anticipated based on a recent investigation[11] of the Ti-Ga phase diagram. The solubility of gallium in α titanium is in fact considerably lower than originally reported. In the 1200°F temperature range, the terminal α solid solution boundary actually exists at about 7 wt pct Ga as compared to the previous estimate of 14 to 15 wt pct. The fatigue precracked Charpy tests show all the alloys, including the A1 composition with an aluminum equivalent of only 6.4, are in fact unstable in the as-heat-treated condition. However, the toughness for the alloys of lower α stabilizer content remains above the critical fracture toughness level after thermal exposures to 1000 hr at 1000°F which is necessary to cause severe embrittlement in the post-creep tensile test.

The fatigue precrack Charpy thermal-stability study on the C1 alloy gave an activation energy of 45 kcal per g-mole which is in agreement with that reported[11] for mutual diffusion between Ti_3Ga and α titanium. However, it remains to be explained why these values should be in agreement considering the presence of aluminum and tin in these alloys. Aluminum and tin are recognized[16] to have interdiffusion activation energies in titanium of the order of 25 kcal per g-mole. The present data show a slower diffusion for gallium in titanium at lower temperatures, as compared to that of aluminum and tin. The superior thermal stability

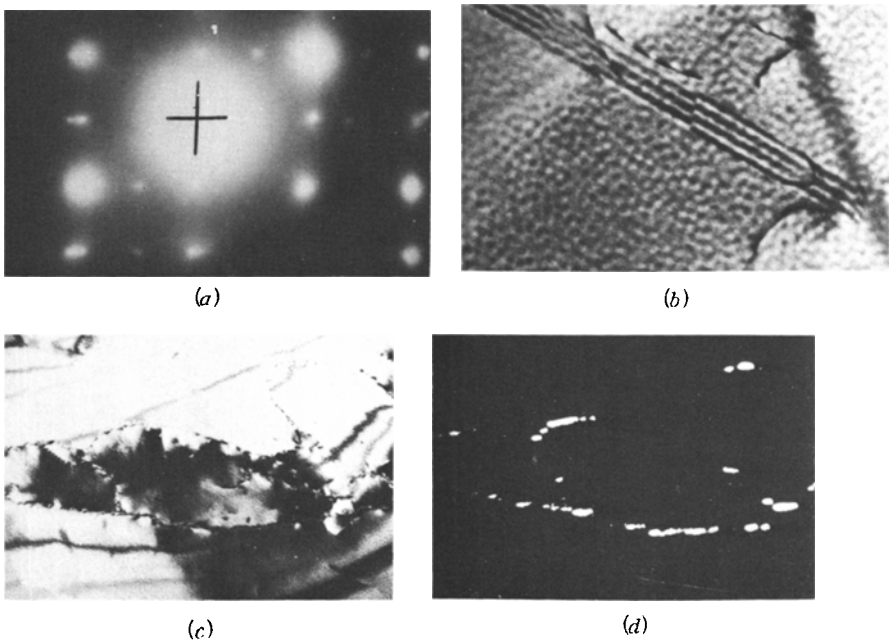

Fig. 9—Electron transmission results for the C1 alloy identifying the location of the Ti_3Al and Zr_5Si_3 phases. (*a*) Electron diffraction pattern, Ti_3(Al, Sn, Ga), $2\bar{1}\bar{1}0$ zone axis; (*b*) bright field, magnification 39,250 times, proposed Ti_3(Al, Sn, Ga) location; (*c*) bright field, magnification 11,775 times; (*d*) dark field, magnification 11,775 times. Zr_5Si_3 at grain boundaries.

for these gallium containing alloys would be expected in the lower temperature range (<1000°F) simply resulting from the slower interdiffusion rates.

CONCLUSIONS

Gallium additions to titanium alloys were confirmed to be about 80 pct as effective in strengthening as aluminum on a weight percent basis, although the alloys containing gallium were not as stable as previously anticipated.

The factors which exert a major influence on the elevated temperature creep resistance are the α stabilizer concentration, the silicon content and the elevated temperature yield strength. An hypothesis for the superior creep resistance for the C1 alloy is suggested to be that of dispersion strengthening of the α phase by the ordered Ti_3X phase and pinning of the interplatelet and β grain boundaries by a Zr_5Si_3 precipitate.

The formation of the Ti_3X phase is presumed responsible for the metallurgical instability in these alloys, but its presence is necessary to achieve the superior creep resistance. The kinetics of embrittlement at temperatures below 1000°F for the gallium containing titanium alloys is apparently slower than that for commercial alloys containing only aluminum and tin which may be associated to the slower interdiffusion rate of gallium in titanium as compared to these other elements.

The correlation of the fatigue precracked Charpy K_c test data with these from the post-creep tensile ductility results shows the former, a K_c or a fracture mechanics related test, to be the more sensitive monitor of metallurgical stability in titanium-base alloys.

ACKNOWLEDGMENTS

The authors wish to acknowledge the assistance of R. W. Smashey for the selected area electron transmission and electron diffraction phase identification portions of this study. The sponsorship of this study under the Air Force Contract F-33-615-69-C-1423 by AFML/MAMP is also gratefully acknowledged.

REFERENCES

1. F. A. Crossley and W. F. Carew: *AIME Trans.*, 1957, vol. 209, pp. 43-46.
2. P. J. Soltis: *Trans. TMS-AIME*, 1965, vol. 233, pp. 903-10.
3. C. E. Shamblen: *Met. Trans.*, 1971, vol. 2, pp. 277-80.
4. E. Ence and H. Margolin: *Trans. TMS-AIME*, 1961, vol. 221, pp. 151-57.
5. D. Clark, K. Jepson, and G. Lewis: *J. Inst. Metals*, 1965, vol. 91, pp. 197-203.
6. F. A. Crossley: *Trans. TMS-AIME*, 1966, vol. 236, pp. 1174-85.
7. M. J. Blackburn: *Trans. TMS-AIME*, 1967, vol. 236, pp. 1200-08.
8. R. P. Elliot: *Constitution of Binary Alloys, First Supplement*, p. 459 and p. 829, McGraw-Hill Book Co., New York, 1965.
9. H. W. Rosenberg: *The Science, Technology and Application of Titanium*, 1st ed., R. I. Jaffee and N. E. Promisel, eds., pp. 851-60, Pergamon Press, Oxford, 1970.
10. K. S. Jepson, L. Larke and C. A. Stubbington: *The Science, Technology and Application of Titanium*, 1st ed., R. I. Jaffee and N. E. Promisel, eds., pp. 861-74, Pergamon Press, Oxford, 1970.
11. C. E. Shamblen and C. J. Rosa: *Met. Trans.*, 1971, vol. 2, pp. 1925-31.
12. S. R. Seagle and H. B. Bomberger: *The Science, Technology and Application of Titanium*, 1st ed., R. I. Jaffee and N. E. Promisel, eds., pp. 1001-08, Pergamon Press, Oxford, 1970.
13. F. R. Larson and J. Miller: *Trans. ASME*, 1952, vol. 74, pp. 765-71.
14. C. Wert and C. Zener: *J. Appl. Phys.*, 1950, vol. 21, pp. 5-8.
15. R. L. Orr, O. D. Sherby, and J. E. Dorn: *Trans. ASM*, 1954, vol. 46, pp. 113-28;
16. D. Goold: *J. Inst. Metals*, 1959, vol. 88, pp. 444-48.

Corrections to *Met. Trans.*, 1972 vol. 3

Thermodynamic Properties and Electrical Conductivity of Ta_3N_5 and TaON, by J. H. Swisher and M. H. Read, pp. 489–94.

Page 493, Fig. 5

The abscissa in Fig. 5 should read

$\log (p_{N_2})^{1/2}$ rather than $\log p_{N_2}$

The equation in Fig. 5 should read

$\int N_N d \log (p_{N_2})^{1/2} = 0.789$